

## Breakup mechanisms for ${}^7\text{Li} + {}^{197}\text{Au}$ , ${}^{204}\text{Pb}$ systems at sub-barrier energies

D.H. Luong<sup>1,a</sup>, M. Dasgupta<sup>1</sup>, D.J. Hinde<sup>1</sup>, R. du Rietz<sup>1,b</sup>, R. Rafiei<sup>1,c</sup>, M. Evers<sup>1</sup>, C.J. Lin<sup>1,d</sup>, A. Wakhle<sup>1</sup>, K. Ramachandran<sup>1,2</sup>, I.P. Carter<sup>1</sup>, and A. Diaz-Torres<sup>3</sup>

<sup>1</sup>Department of Nuclear Physics, The Australian National University, ACT 0200, Australia

<sup>2</sup>Nuclear Physics Division, Bhabha Atomic Research Centre, Trombay, Mumbai 400085, India

<sup>3</sup>ECT\*, Villa Tambosi, I-38123 Villazzano, Trento, Italy

**Abstract.** Coincidence measurements of breakup fragments were carried out for the  ${}^7\text{Li} + {}^{197}\text{Au}$  and  ${}^{204}\text{Pb}$  systems at sub-barrier energies. The mechanisms triggering breakup, and time-scales of each process, were identified through the reaction Q-values and the relative energy of the breakup fragments. Binary breakup of  ${}^7\text{Li}$  were found to be predominantly triggered by nucleon transfer, with  $p$ -pickup leading to  ${}^8\text{Be} \rightarrow \alpha + \alpha$  decay being the preferred breakup mode. From the time-scales of each process, the coincidence yields were separated into prompt and delayed components, allowing the identification of breakup process important in the suppression of complete fusion of  ${}^7\text{Li}$  at above-barrier energies.

### 1 Introduction

The discovery of halo nuclei [1, 2] ushered in the development of radioactive ion beams (RIBs). This called for better understanding of the interactions of their cousins, the weakly-bound but stable nuclei. Such understanding is essential in relating the internal nuclear structure, e.g. nucleon clustering and low threshold for cluster-breakup [3–6], to the reaction outcomes, e.g. fusion, nucleon transfer, and breakup [7]. Relating nuclear structure of weakly-bound and unstable nuclei to nuclear reaction outcomes within a coherent framework has become an important goal in reaction theory. With  ${}^6,{}^7\text{Li}$  and  ${}^9\text{Be}$  being more accessible, while offering similar characteristics (namely nucleon clustering and low breakup threshold), studying the former presents a great opportunity to understand and predict the behaviour of the much less accessible RIBs.

Complete fusion (CF) of the weakly-bound nuclei  ${}^6,{}^7\text{Li}$  and  ${}^9\text{Be}$  with high- $Z$  targets, at above-barrier energies, are consistently observed [8–10] to be lower than theoretical expectation. The low threshold energies for breakup of Li and Be are widely associated with this suppression of CF [8–13], with breakup described as cluster decay from unbound states independent of the mechanism that populates it [14–20]. Qualitatively, coupling to channels leading to breakup was shown [21] to suppress CF at above-barrier energies. More realistic modelling of the inter-

play between breakup and CF requires the incorporation of the mechanisms for triggering breakup, the time-scales of breakup [22–24], and possible post-breakup capture of the fragments [7, 25]. To isolate breakup itself from the probability of fragment capture, sub-barrier coincidence measurements of breakup fragments of  ${}^7\text{Li}$  with  ${}^{197}\text{Au}$  and  ${}^{204}\text{Pb}$  were performed. The mechanisms for breakup, and their time-scale, were identified through the reaction Q-values and the relative energy of the captured breakup fragments.

### 2 Experimental setup

Beams of  ${}^7\text{Li}$  were provided by the 14UD electrostatic accelerator at the Australian National University. They were incident on a self-supporting  ${}^{197}\text{Au}$  target,  $150 \mu\text{g cm}^{-2}$  in thickness, and a  $400 \mu\text{g cm}^{-2}$  thick  ${}^{204}\text{Pb}$  target on a  $20 \mu\text{m cm}^{-2}$  carbon backing. The beam energies and target combination are listed in Table 1, along with the centre-of-mass barrier energy  $V_b$  of each reaction.

**Table 1.** Beam energies at which measurements were made for the reactions of  ${}^6\text{Li}$  with indicated targets.  $E_{\text{c.m.}}$  includes energy loss in the target.

Target	$V_b$ (MeV)	$E_{\text{beam}}$ (MeV)	$E_{\text{c.m.}}$ (MeV)	$E/V_b$
${}^{197}\text{Au}$	28.72 <sup>†</sup>	28.0	27.00	0.94
		29.0	27.97	0.97
${}^{204}\text{Pb}$	29.54 <sup>†</sup>	27.5	26.54	0.90
		30.0	28.96	0.98

<sup>†</sup> Scaled barrier as described in Ref. [26].

<sup>a</sup>e-mail: huy.luong@anu.edu.au

<sup>b</sup>Present address: Malmö University, Faculty of Technology and Society, 205 06 Malmö, Sweden

<sup>c</sup>Present address: School of Electrical, Electronic and Computer Engineering, The University of Western Australia, Perth, WA 6009, Australia

<sup>d</sup>Present address: China Institute of Atomic Energy, Beijing 102413, P.R. China

Charged breakup fragments from the reaction were captured in coincidence using BALiN [27], a detector array consisting of four large area double-sided silicon strip detectors (DSSD) arranged in a lamp-shade configuration with apex angle  $45^\circ$ . For the given detector thickness of  $400 \mu\text{m}$ , only high- $Z$  particles,  $\alpha$ -particles, and low energy protons ( $<7.0 \text{ MeV}$ ), deuterons ( $<9.0 \text{ MeV}$ ) and tritons ( $<11.0 \text{ MeV}$ ) would fully deposit their energies in the DSSDs. The detector array was placed at backward angles, covering scattering angles from  $117^\circ$  to  $167^\circ$ . The pixel identification characteristics of the DSSDs does not allow position location within the pixel. However, to simplify subsequent event reconstruction, a position was assumed by randomisation, taking a uniform distribution of the position within the physical boundaries of the pixel.

### 3 Mechanism for binary breakup

The Verification of the identities of the coincidence particles, and thus the reaction mechanism, requires the reconstruction of the three-body reaction  $Q$ -value. Consider a two-body collision with a projectile having initial and final kinetic energy  $E_{\text{lab}}$  and  $E_f$ , respectively. The ground-state  $Q$ -value,  $Q_{\text{gg}}$ , for any collision can be written as

$$Q_{\text{gg}} = E_f + E_{\text{ex,PL}} + E_{\text{ex,TL}} + E_{\text{rec}} - E_{\text{lab}}, \quad (1)$$

where  $E_f$  is the kinetic energy of the projectile-like nuclei,  $E_{\text{ex,PL}}$  and  $E_{\text{ex,TL}}$  are the excitation energies of the projectile-like and target-like nuclei respectively, and  $E_{\text{rec}}$  is the recoil energy of the latter, all in the laboratory frame. For binary breakup of the projectile-like nucleus, its excitation energy is shared by the kinetic energies  $E_i$  of the fragments,  $E_f + E_{\text{ex,PL}} = E_1 + E_2$ , and the reaction  $Q$ -value can be determined from energy balance as

$$Q = E_1 + E_2 + E_{\text{rec}} - E_{\text{lab}}, \quad (2)$$

where  $E_{\text{lab}}$  is derived from  $E_{\text{beam}}$  after correcting for energy lost in traversing the target. The recoil energy  $E_{\text{rec}}$  and mass of the target-like nucleus is determined through conservation of momentum from the momenta and masses of the two detected fragments [24, 28]. Since the excitation energy  $E_{\text{ex,TL}}$  of the target-like nucleus cannot be captured in our detector, the  $Q$ -spectra will show separate peaks for each state populated in the target-like nucleus.

Shown in Fig. 1 are the reconstructed  $Q$ -spectra, not corrected for coincidence detection efficiency, for the reactions of  ${}^7\text{Li}$  with  ${}^{197}\text{Au}$  and  ${}^{204}\text{Pb}$ . The spectra show that almost all the yield contributes to sharp peaks in  $Q$ , meaning the breakup is indeed almost exclusively binary, with identified breakup modes of  $\alpha + \alpha$  (green),  $\alpha + t$  (blue), and  $\alpha + d$  (magenta). The expected  $Q_{\text{gg}}$  for respective breakup modes are indicated by dashed lines.

Direct breakup of  ${}^7\text{Li}$  into  $\alpha + t$  can be seen to be less probable than breakup triggered by nucleon transfer, e.g.  $n$ -stripping of  ${}^7\text{Li}$  leading to  ${}^6\text{Li} \rightarrow \alpha + d$ , and  $p$ -pickup resulting  ${}^8\text{Be} \rightarrow \alpha + \alpha$ . Peaks in the  $Q$ -spectra corresponding to  $\alpha + \alpha$  breakup show that the target-like products  ${}^{196}\text{Pt}$  and  ${}^{203}\text{Tl}$  are populated mostly in their excited states. For

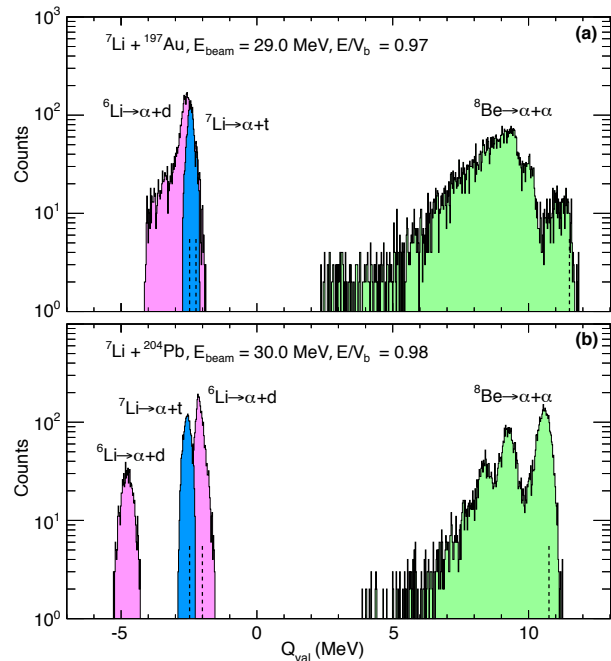


**Figure 1.**  $Q$ -spectra determined for the reactions of  ${}^7\text{Li}$  with  ${}^{197}\text{Au}$  and  ${}^{204}\text{Pb}$  at indicated energies. Identified breakup modes consist  $\alpha + d$  (magenta) and  $\alpha + \alpha$  (green). Dashed lines indicate the expected  $Q_{\text{gg}}$  for each breakup mode. Peaks in the  $Q$ -spectra indicate breakup following the population of excited states of the target-like nuclei. (Contribution from  $\alpha + p$  are not plotted due to their insignificant yield.)

the  $n$ -stripping reaction of  ${}^7\text{Li}$  with  ${}^{204}\text{Pb}$ , the higher  $E_{\text{beam}}$  allowed population of  ${}^{205}\text{Pb}$  at up to  $\approx 2.7 \text{ MeV}$  excitation.

The  $Q$ -value spectra give no clue to the relative population between the ground- and excited-states of  ${}^8\text{Be}$  and  ${}^6\text{Li}$ . However, the energy  $E_{\text{ex,PL}}$  of the excited states of the target-like nuclei appears in the kinetic energies  $E_{1,2}$  of the breakup fragments, and have been shown [24] to be related to the time-scales of the process.

### 4 Time-scale of breakup and $E_{\text{rel}}$

For binary breakup of the projectile-like nucleus on the outgoing trajectory, the relative energy  $E_{\text{rel}}$  of the fragments is the sum  $Q_{\text{BU}} + E_{\text{ex,PL}}$ , where  $Q_{\text{BU}}$  is the breakup  $Q$ -value. In terms of measured quantities

$$E_{\text{rel}} = \frac{m_2 E_1 + m_1 E_2 - 2 \sqrt{m_1 E_1 m_2 E_2} \cos \theta_{12}}{m_1 + m_2}, \quad (3)$$

where  $\theta_{12}$  is the angular separation between the fragments. For breakup close to the target nucleus, the breakup fragments particles will experience tidal effect [29] and  $E_{\text{rel}}$  no longer depends solely on the breakup energetics.

#### 4.1 Relating fragment relative energy to time-scale of breakup

Using the three-body three dimensional model PLATYPUS [30–32], an illustrative calculation of the

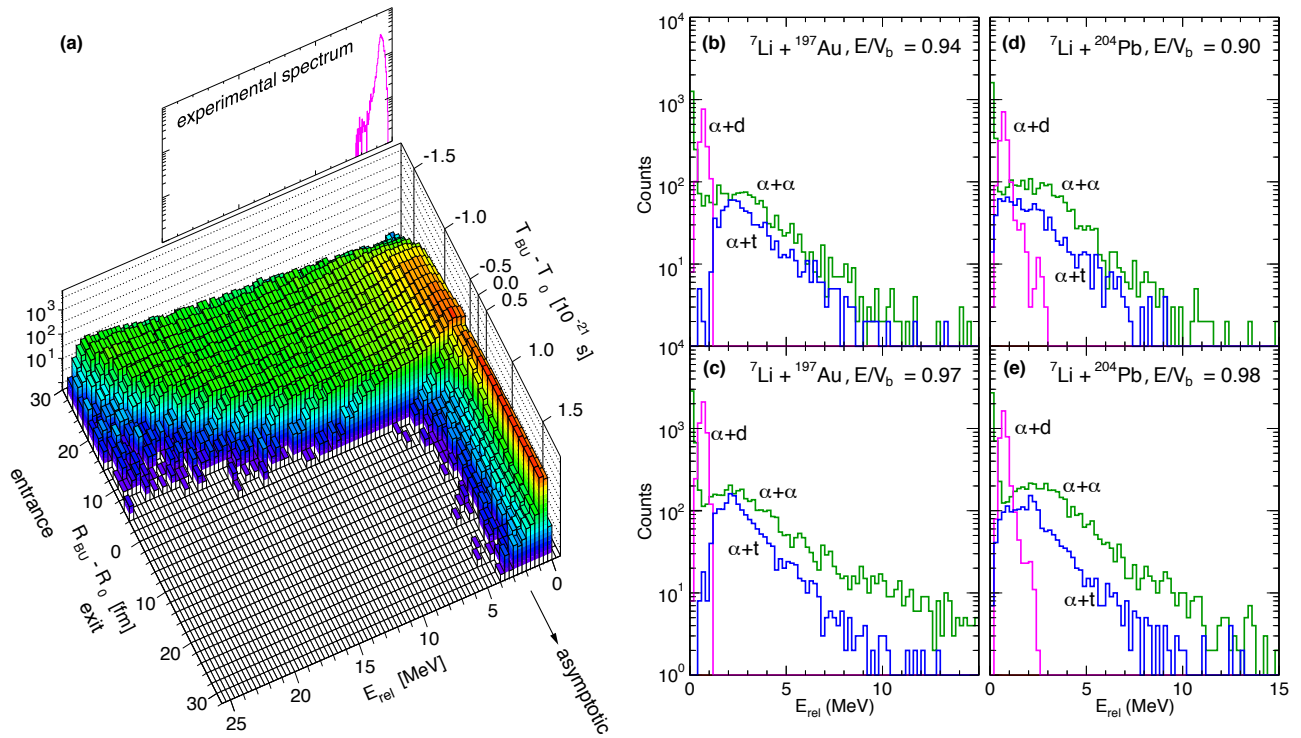


**Figure 2.** (a) Landscapes of the classically calculated  $E_{\text{rel}}$  versus the nuclear separation (left axis) or time (right axis) at which breakup occurs, relative to the point of closest approach ( $R_0$ ,  $T_0$ ), for  ${}^6\text{Li} \rightarrow \alpha + d$  breakup in the field of a  ${}^{207}\text{Pb}$  nucleus. The spread in  $E_{\text{rel}}$  arises from the different impact parameters and fragments orientations at the moment of breakup. Breakup prior to reflection,  $(T_{\text{BU}} - T_0) < 0$  results in higher  $E_{\text{rel}}$  values than breakup after reflection  $(T_{\text{BU}} - T_0) > 0$ . Impact parameters corresponding to angular momenta up to  $49\hbar$  were considered. (b–e) Experimental  $E_{\text{rel}}$  spectra for identified  $\alpha + \alpha$  (green),  $\alpha + t$  (blue), and  $\alpha + d$  (magenta) breakup modes for the indicated reactions. These spectra have neither been corrected for events with incomplete energy deposition, nor for coincidence detection efficiency.

dependence of  $E_{\text{rel}}$  on the projectile-target separation at which breakup occurs ( $R_{\text{BU}}$ ) was performed for breakup of  ${}^6\text{Li}$  from the  $3^+$  (2.186 MeV) state. The distance  $R_{\text{BU}}$  was *uniformly* sampled along the trajectory of the  ${}^6\text{Li}$  projectile with energy  $E_{\text{beam}} = 29.0$  MeV. The orientations of the  $\alpha + d$  fragments at  $R_{\text{BU}}$ , relative to the target nucleus, were also randomly sampled with an isotropic distribution. Shown in Fig. 2 is the result of this calculation. Since this is a classical calculation, the time of breakup  $T_{\text{BU}}$  relative to that of the closest approach ( $T_0$ ) could be exactly evaluated, and is also shown. For comparison, the one-dimensional experimental  $E_{\text{rel}}$  spectra for  $\alpha + d$  coincidences, from breakup of  ${}^6\text{Li}$  on  ${}^{205}\text{Pb}$  following  $n$ -stripping of  ${}^7\text{Li}$  at  $E_{\text{beam}} = 30.0$  MeV, is shown above in magenta.

The variation of  $E_{\text{rel}}$  as a function of  $R_{\text{BU}} - R_0$  is indicative of the dependence of the former on the latter. The wide spread of  $E_{\text{rel}}$  from breakup before reaching  $R_0$  is due to post-breakup acceleration of the fragments in the Coulomb field of the target nucleus. For breakup after the projectile-like nucleus has travelled past  $R_0$ ,  $E_{\text{rel}}$  converges to  $\approx 0.7$  MeV, the energy available at breakup. The mapping of radius  $R_{\text{BU}}$  to the breakup time  $T_{\text{BU}}$  allows correlation of the time-scale for breakup to the measured  $E_{\text{rel}}$ . Given that transfer occurs on time-scales of  $\sim 10^{-22}$  s [24], information on  $T_{\text{BU}}$  allows the classification of breakup

into *prompt* ( $T_{\text{BU}} \lesssim 10^{-22}$  s), or *delayed* breakup. Prompt breakup results in breakup of the projectile or projectile-like nuclei in the entrance trajectory, and thus reduces the flux of intact nuclei available for fusion at the distance of closest approach  $R_0$ . On the other hand, delayed breakup happens on the exit trajectory, in the asymptotic region. These nuclei have survived breakup at  $R_0$ , and thus would have been able to participate in fusion if the beam energy was above the barrier.

## 4.2 Separation of prompt and delayed breakup

From the established relationship between the  $E_{\text{rel}}$  spectrum and the time-scale of breakup (Fig. 2(a)), the experimental  $E_{\text{rel}}$  spectra shown in Fig. 2(b–e) thus give information on the breakup time-scale, allowing a degree of separation between *prompt* and *delayed* breakup. For the direct  ${}^7\text{Li} \rightarrow \alpha + t$  breakup, the broad distribution to high  $E_{\text{rel}}$  shows its prompt nature, and would possibly play a role in the suppression of CF at above-barrier energies. For breakup at higher  $E_{\text{beam}}$ , there is a slight peak at  $E_{\text{rel}} \sim 2.1$  MeV, perhaps denoting a tiny fraction of breakup from the  ${}^7_2^-$  (4.65 MeV) state of  ${}^7\text{Li}$  whose lifetime of  $\sim 9 \times 10^{-21}$  s might just be long enough to see the projectile breakup in the asymptotic region.

For transfer-triggered breakup, the breakup of  ${}^6\text{Li} \rightarrow \alpha + d$  following  $n$ -stripping have mostly high concentration of events with  $E_{\text{rel}} = 0.7$  MeV. This indicates breakup in the asymptotic region, and would have little impact in the CF of  ${}^7\text{Li}$  at above-barrier energies. As for the  ${}^8\text{Be} \rightarrow \alpha + \alpha$  breakup following  $p$ -pickup, the high intensity of events with  $E_{\text{rel}} \approx 0.1$  MeV and broad tails comprising high  $E_{\text{rel}}$  events follows qualitatively the behaviour of asymptotic and prompt breakup, respectively, as expected from the classical model (Fig. 2(a)). Even when the asymptotic (low  $E_{\text{rel}}$ ) component is excluded, prompt  $\alpha + \alpha$  breakup is still the most probable binary breakup channel for  ${}^7\text{Li}$ . This reaction channel would thus play a major role in the suppression of CF, at above-barrier energies, in  ${}^7\text{Li}$ -induced reactions.

## 5 Conclusion

The measurements presented in this work carry the most complete information on breakup in the reactions of  ${}^7\text{Li}$  with high- $Z$  targets. Binary breakup of  ${}^7\text{Li}$  projectile is found to be triggered predominantly by nucleon transfer, both  $n$ -stripping leading to the  $\alpha + d$  breakup of  ${}^6\text{Li}$ , and  $p$ -pickup triggering the  ${}^8\text{Be} \rightarrow \alpha + \alpha$  decay. The dominance of transfer-initiated breakup is a stark contrast to the expected  $\alpha + \text{triton}$  cluster breakup of  ${}^7\text{Li}$ . This will provide a major challenge for the quantum theory of low energy nuclear reactions. From the relative energy  $E_{\text{rel}}$  of the binary breakup fragments, information on the breakup time-scales allows the separation of prompt and asymptotic breakup components. By incorporating the breakup time-scale into classical model calculations like PLATYPUS, more quantitative understanding of the breakup mechanism and its effects on fusion are expected.

## References

- [1] I. Tanihata *et al.*, Phys. Lett. **160B**, 380 (1985)
- [2] I. Tanihata *et al.*, Phys. Rev. Lett. **55**, 2676 (1985)
- [3] E. Rutherford *et al.*, Phil. Mag. **42**, 809 (1921)
- [4] J. A. Wheeler, Phys. Rev. **52**, 1083 (1937)
- [5] R. W. Ollerhead *et al.*, Phys. Rev. **134**, B74 (1963)
- [6] O. Häusser *et al.*, Phys. Lett. B **38**, 75 (1972)
- [7] L. F. Canto *et al.*, Phys. Rep. **424**, 1 (2006)
- [8] M. Dasgupta *et al.*, Phys. Rev. C **66**, 041602(R) (2002)
- [9] M. Dasgupta *et al.*, Phys. Rev. C **70**, 024606 (2004)
- [10] S. Thakur *et al.*, EPJ Web of Conf. **17**, 16017 (2011)
- [11] M. Dasgupta *et al.*, Phys. Rev. Lett. **82**, 1395 (1999)
- [12] C. Signorini *et al.*, Eur. Phys. J. A **5**, 7 (1999)
- [13] Y. W. Wu *et al.*, Phys. Rev. C **68**, 044605 (2003)
- [14] H. Freiesleben *et al.*, Phys. Rev. C **10**, 245 (1974)
- [15] G. R. Kelly *et al.*, Phys. Rev. C **63**, 024601 (2000)
- [16] R. Ost *et al.*, Z. Phys. **266**, 369 (1974)
- [17] J. L. Québert *et al.*, Phys. Rev. Lett. **32**, 1136 (1974)
- [18] D. Scholz *et al.*, Nuc. Phys. A **288**, 351 (1977)
- [19] C. Signorini *et al.*, Phys. Rev. C **67**, 044607 (2003)
- [20] A. Shrivastava *et al.*, Phys. Lett. B **633**, 463 (2006)
- [21] K. Hagino *et al.*, Phys. Rev. C **61**, 037602 (2000)
- [22] D. J. Hinde *et al.*, Phys. Rev. Lett. **89**, 272701 (2002)
- [23] R. Rafiei *et al.*, Phys. Rev. C **81**, 024601 (2010)
- [24] D. H. Luong *et al.*, Phys. Lett. B **695**, 105 (2011)
- [25] A. Shrivastava *et al.*, Phys. Lett. B **718**, 931 (2013)
- [26] E. F. Aguilera *et al.*, Phys. Rev. C **80**, 044605 (2009)
- [27] D. H. Luong *et al.*, PoS(NIC XII) 185 (2012)
- [28] D. H. Luong *et al.*, EPJ Web of Conf. **35**, 05007 (2012)
- [29] A. B. McIntosh *et al.*, Phys. Rev. Lett. **99**, 132701 (2007)
- [30] A. Diaz-Torres *et al.*, Phys. Rev. Lett. **98**, 152701 (2007)
- [31] A. Diaz-Torres, J. Phys. G: Nucl. Part. Phys. **37**, 075109 (2010)
- [32] A. Diaz-Torres, Comput. Phys. Commun. **182**, 1100 (2011)